



Article

K X-ray Emission for Slow Oxygen Ions Approaching a Copper Metal Surface

Zhangyong Song^{1,2,*} , Xuan Liu³, Mingwu Zhang^{1,2}, Junkui Xu^{1,2}, Yong Feng^{1,2}, Bingzhang Zhang^{1,4}, Wei Wang^{1,2}, Junliang Liu^{1,2}, Caojie Shao^{1,2} , Deyang Yu^{1,2}, Yanling Guo³ and Lin Chen^{3,*}

¹ Institute of Modern Physics, Chinese Academy of Sciences, Lanzhou 730000, China

² School of Nuclear Science and Technology, University of Chinese Academy of Sciences, Beijing 100049, China

³ School of Nuclear Science and Technology, Lanzhou University, Lanzhou 730000, China

⁴ School of Nuclear Science and Technology, University of South China, Hengyang 421001, China

* Correspondence: songzhy@impcas.ac.cn (Z.S.); chenlin@lzu.edu.cn (L.C.)

Abstract: We report on the K X-ray emission for 9–140 keV oxygen ions with initial charge states from 3 to 7 approaching a copper surface. The peak center of the measured X-ray spectrum slightly shifts towards higher energies with the increasing of the initial charge state of the incident ions. For the collisions of oxygen ions with no K-vacancies ($q = 3\text{--}6$), the X-ray yield per incident ion increases gradually with the projectile's kinetic energy, while for the O^{7+} ions (with a K-vacancy) it is nearly independent of the energy. The K-shell ionization cross-sections for the oxygen ions with no K-vacancies obtained from the experiments are well consistent with the calculations of the binary encounter approximation model when the collision energy is larger than 30 keV, whereas they are several times larger than the theoretical values at collision energies of less than 30 keV.

Keywords: highly charged ions; X-ray emission; spectrum shifts



Citation: Song, Z.; Liu, X.; Zhang, M.; Xu, J.; Feng, Y.; Zhang, B.; Wang, W.; Liu, J.; Shao, C.; Yu, D.; et al. K X-ray Emission for Slow Oxygen Ions Approaching a Copper Metal Surface. *Atoms* **2022**, *10*, 124. <https://doi.org/10.3390/atoms10040124>

Academic Editors: Izumi Murakami, Daiji Kato, Hiroyuki A. Sakaue and Hajime Tanuma

Received: 21 September 2022

Accepted: 24 October 2022

Published: 26 October 2022

Publisher's Note: MDPI stays neutral with regard to jurisdictional claims in published maps and institutional affiliations.



Copyright: © 2022 by the authors. Licensee MDPI, Basel, Switzerland. This article is an open access article distributed under the terms and conditions of the Creative Commons Attribution (CC BY) license (<https://creativecommons.org/licenses/by/4.0/>).

1. Introduction

In the past decades, the interaction between highly charged ions (HCIs) with solid surfaces has received extensive attention [1–4]. A large number of experiments have been carried out in low-energy regions, particularly where the incident velocity is less than the Bohr velocity. Researchers are very concerned about the effects of the incident ion's charge state and kinetic energy in impacting processes because of the formation and de-excitation of “hollow atoms” [1]; the ionization of the inner shell of target atoms plays an important role in astrophysics and high energy density physics. In addition, the interaction of HCIs with solid surfaces provides new insights into materials [5] and life sciences [6], and the applications of HCIs have important prospects in surface analysis, surface modification, and microelectronic preparation processes [7].

In the early stage, due to the limitation of ion sources and detection technology, experimental research in this field primarily focused on low charge state ions. In 1954, Hagstrum proposed that the charge exchange in the interaction of HCIs with metal surfaces is completed through a step-by-step electronic transition process [8]. In 1973, Arifov put forward a multi-electron resonance capture mechanism to explain the multi highly excited ions formed as HCIs approached the target surface [9]. Finally, Burgdorfer established a widely accepted classic over-barrier model (COBM) in 1991 [10]. According to this model, a large number of electrons in the conduction band are resonantly captured into the highly excited empty states of the HCIs as they reach a critical distance from the surfaces, forming a hollow atom. The hollow atoms are in unstable multi-excited or highly excited states and are de-excited via auto-ionization, the Auger process, and X-ray emission. In addition to the COBM model, a two-state vector model [11–13] was also proposed to investigate the population probability for the Rydberg states during the neutralization process of the ions on the surfaces. In the aspects of the experiments, Machicoane et al. measured the X-ray

emission by the hollow atoms and investigated the internal two-electron excitation process in the interaction of low-velocity highly charged gold ions with the gold surface [14]. In recent years, with the rapid development of the ion source technology, some laboratories in the United States, Austria, Germany, France, Japan, and China have studied the interaction of various HCIs with metal and insulated solid surfaces using ion beams provided by the electron beam ion source and/or the electron cyclotron resonance ion source.

There are many experimental studies on heavy incident ions with metal targets, but there are few studies on the collision system of light ions with light metal targets. Among them, the O element is abundant in the universe and planets. It is of great significance for studying the evolution of celestial bodies and the mechanism of comet X-ray emission [15–17]. For example, the charge transfer between ions and neutral gases will cause cold celestial bodies to emit X-rays [18]. In the present work, the highly charged O^{q+} ($q = 3-7$) ions with a kinetic energy range from 1.5 to 20 keV/ q are extracted from an electron cyclotron resonance ion source at the Institute of Modern Physics, Chinese Academy of Sciences, to collide with a copper surface. We measured the emitted X-rays and studied the dependence of the X-ray yield on the initial charge state and kinetic energy of the O ions. The ionization cross-sections are also studied.

2. Experiments

The experiment was performed on the atomic physics experiment platform located at the 14.5-GHz ECRIS in the Institute of Modern Physics, Chinese Academy of Sciences. The details of the experimental platform are described elsewhere [19,20]. Briefly, the O^{q+} ($q = 3-7$) ions were extracted from the ECRIS and selected by a 90° analysis magnet. Then, the beam passed through a beam profile device that was used to adjust the beam size and position. The adjusted beam entered a collimating pipe with a length of 600 mm through a slit with a diameter of 10 mm. In the collimating pipe, we used our developed beam density meter (incident aperture of 4 mm, measuring aperture of 2 mm) to measure the beam intensity [20]. Finally, the beam passed through an aperture, 5 mm in diameter, and was delivered to the Cu target, which had a purity of 99.99%, and the beam current was about 3–11 nA. The base pressure in the chamber was maintained at about 1.5×10^{-8} mbar. It should be noted that at this pressure a layer of adsorbed material with one molecular thickness would cover the surface in about 1000 s. In order to sputter the adsorbates, the target surface was scanned by the ion beam with a current of \sim nA at an angle of 20° for about 30 min before the X-ray measurements so that the thickness of the possible adsorbates was no more than one molecular thickness. The emitted X-rays were detected with the use of an ultra-high-performance silicon drift detector (SDD) from the AMPTEK company, placed at 45° to the beam, inside the chamber. Before the experiments, the detector was calibrated using the emitted X-ray lines of the radioisotopes of ^{55}Fe . The detector had an effective detection area of 25 mm^2 and an energy resolution of about 135 eV at 5.9 keV.

3. Results and Discussion

3.1. X-ray Emission for Interaction of Oxygen Ions with No K-Vacancies

Figure 1 shows the measured X-ray spectra for the O^{q+} ($q = 3-6$) ions impinging on the target surface. The kinetic energy range is from 5 to 20 keV/ q for the O^{3+} and O^{5+} ions, and 1.5 to 20 keV/ q for the O^{6+} ions. It can be seen that for collisions of any charge state used in the experiments the X-ray count increases with the increasing of the kinetic energy of the incident oxygen ions. The X-ray count rate also rapidly increases as the charge state of the ions increases. In addition to the oxygen K X-rays, as shown in Figure 1, we also observed the characteristic K X-rays of carbon. The unexpected carbon X-rays are probably due to two reasons. One is related to the collisions of the beam with the target frame, which is made of 304 stainless steel, containing about 0.08% carbon element, and the other is related to the surface oxidization and adsorption of hydrocarbon on the surface. The carbon X-rays may be emitted by the interaction of the ions with the carbon pollutants adsorbed on the target surface.

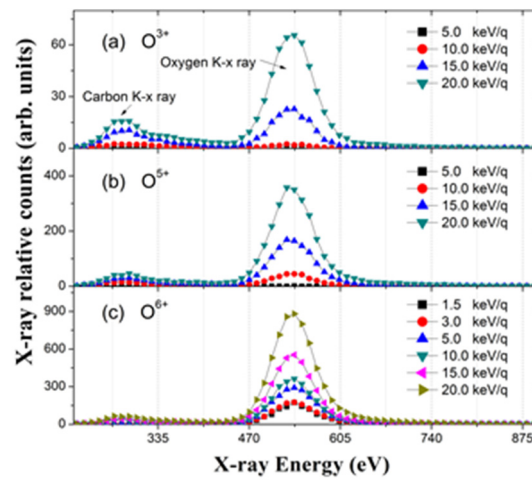


Figure 1. X-ray spectra induced by different kinetic energy O^{q+} ($q = 3, 5, 6$) ions impinging on the Cu surface. (a) O^{3+} ions with incident energy range from 5 to 20 keV/q; (b) O^{5+} ions from 5 to 20 keV/q; (c) O^{6+} ions from 1.5 to 20 keV/q.

The energy shift of the oxygen X-rays is investigated as a function of the initial charge state of the ions. Figure 2 shows the fit to the measured spectra for the collisions of the 10 keV/q oxygen ions with the Gauss function plus a constant background. The fitting results are summarized in Table 1. As shown in Figure 2 and Table 1, the energy position of the X-rays slightly shifts to a higher energy with the charge state of the ions. There are two possible reasons for the observed energy shifts. The most likely one is related to the Doppler effects because of the higher kinetic energy for the ions with a larger charge state. The other is that, with the increasing of the charge state, the binding energy of the K-shell electron is enhanced. Upon the impact of the ions on the target surface, a compact screening cloud is formed around the projectile. This screening effect reduces the binding energy of the K-shell electrons as compared to that of the isolated ions. Therefore, the energy position of the X-rays just slightly shifts toward higher energies.

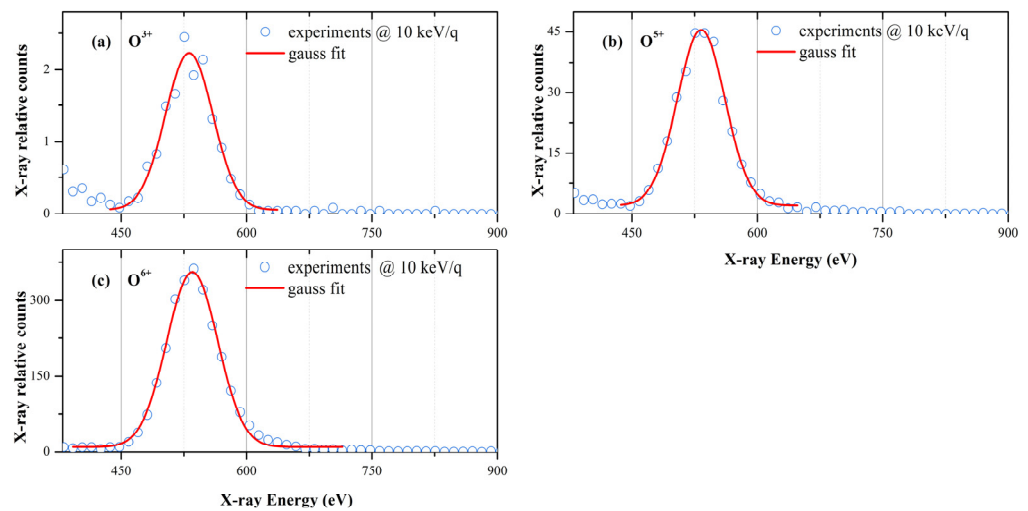


Figure 2. The X-ray spectra in the interaction of O^{q+} ($q = 3, 5, 6$) ions with the Cu surface at kinetic energy of 10 keV/q: (a) O^{3+} , (b) O^{5+} , (c) O^{6+} .

Table 1. Gauss fitting results to the measured X-ray spectra for 10 keV/q oxygen ions with charge state, q, equal to 3, 5, and 6, respectively.

Charge State of Oxygen Ions	Center of the X-ray Peak/eV	Error of the X-ray Peak/eV
3	531.3	1.2
5	532.7	0.5
6	535.0	0.4

For the O^{q+} (q = 3, 5, 6) ions, due to no vacancies existing in the K shell, the K X-rays are certainly generated by the close collisions between the ions and the target atoms below the surface. Assuming the oxygen X-rays are emitted isotropically, the X-ray yield per incident particle can be deduced from the following formula,

$$Y(E) = \frac{N_X}{N_P} \frac{4\pi}{\Omega} \frac{1}{\epsilon\mu}. \tag{1}$$

Here, N_X is the total K X-ray count, and N_P is the total count of the incident ions, which is determined online by the beam density meter (more details about this beam density meter please refer to Ref. [20]). The solid angle Ω seen by the detector from the target surface was 0.004 sr. To minimize the error of the solid angle as far as possible, the beam spot size on the target is always adjusted to be about 2.0 mm for any charge state and energy of the beam used in the experiments. The detector efficiency ϵ of the detector was calculated by using the manufacturer’s specifications. It was 0.294 for the O K-shell X-rays. The μ stands for the absorption coefficient, which is neglected since the detector is placed in a vacuum. The uncertainties of the X-ray yield mainly result from the number of incident ions (~10%), the X-ray counts (~5%), the efficiency of the detector (~3%), and the solid angle (~2%).

The range of the 9–120 keV oxygen ions in the Cu target is about 10 to 120 nm, which is much less than the thickness of the target used in the present experiments; therefore, the target can be considered a thick target. Therefore, the K-shell ionization cross-sections of the oxygen can be derived from the measured X-ray yield using the formula for the thick target [21],

$$\sigma_I(E) = \frac{1}{N\bar{\omega}} \left[\frac{dE}{dR} \frac{dY(E)}{dE} + \mu \frac{\cos\theta}{\cos\varphi} Y(E) \right], \tag{2}$$

where N is the target atom density; $\bar{\omega}$ is the fluorescence yield for the O K X-rays, which is equal to 0.007 [22]; θ is the angle between the beam and the normal direction of the target surface; φ is the angle between the detector direction and the normal target; and μ is the self-absorption coefficient of the Cu target for its own X-rays. The stopping power dE/dR can be calculated using the SRIM program [23]. $dY(E)/dE$ is the slope of the X-ray yield versus the incident ion energy, which is obtained firstly by fitting the polynomials to $ln(E)$ and $ln(Y(E))$ and then calculating it according to the formula $\frac{dY}{dE} = \frac{Y}{E} \frac{d(lnY)}{d(lnE)}$.

The obtained ionization cross-sections are shown in Figure 3. The results of the BEA model, in which the united atom approximation is taken into account, are also plotted [24]. In the BEA model, the electrons are regarded as free electrons, and the ionization process is regarded as a two-body Coulomb scattering between the ion and a free electron. As shown, the ionization cross-section is basically independent of the initial charge state of the ions and gradually increases with the collision energy. These facts indicate that the ionization process is caused by the close collisions of the ions with the target atom below the surface, and at the time of the ionization process, the incident ions reach an equilibrium charge state. The calculations of the BEA model are consistent with the experimental results when the incident energy is larger than 30 keV, whereas a large discrepancy exists at low collision energies, especially in the case of O⁶⁺. It means that other mechanisms should be taken into account to explain this low-energy discrepancy.

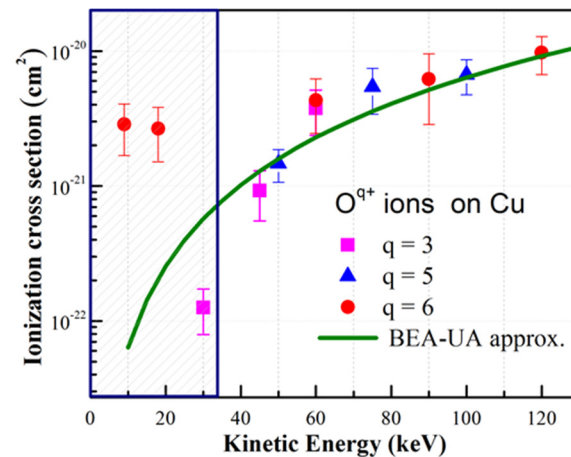


Figure 3. Measured K-shell ionization cross–sections for O^{q+} ions impinging on the Cu surface. The calculation of BEA with the united atom approximation is also shown.

3.2. X-ray Emission for Interaction of Oxygen Ions with A K-Vacancy

Figure 4 shows the measured X-ray spectra for the collisions of the O^{7+} ions, with kinetic energies ranging from 3 to 20 keV/q. The raw X-ray spectra have been normalized into X-ray intensity spectra in units per 10^{12} ions. The X-ray intensity is almost independent of the projectile kinetic energy, and compared with the X-rays induced by the collisions of no-K-vacancy oxygen ions, it is enhanced by more than 95%. For the O^{7+} ions, the electron configuration is 1 s, which means a vacancy in the K shell. When such ions approach the copper surface, they capture electrons at a critical distance from the conduction band, forming the above-surface hollow atoms. The main quantum number of the highest electron occupation is estimated to be 9 according to the COBM. The formed hollow atoms, within an fs time scale, de-excite to the inner shells by X-ray emission and the Auger decay processes before penetrating into the bulk. This case is very different from the X-ray emission of incident ions without the K-vacancy, as was discussed in Section 3.1. Therefore, as the kinetic energy of the incident ions increases, the velocity becomes faster; then, the interaction time with the Cu surface becomes shorter. The measured X-ray yield for the case of the O^{7+} ions should decrease slowly. Taking into account the experimental errors, the independence of the X-ray intensity on the kinetic energy is credible.

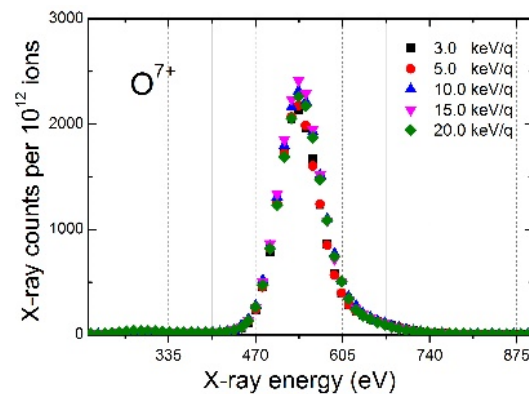


Figure 4. Measured X-ray spectra for O^{7+} ions impinging on the Cu surface at projectile kinetic energies from 3.0 to 20.0 keV/q. The raw X-ray spectra have been normalized into intensity spectra in units per 10^{12} ions.

4. Conclusions

We have measured the K X-ray emission in the interaction between highly charged O^{q+} ($q = 3-7$) ions and the Cu surface in the energy range from 1.5 to 20 keV/q. For the interaction of no-K-vacancy ions, the X-ray yield and ionization cross-section increase with

the kinetic energy of the ions. However, the X-ray intensity induced by the oxygen ions with a *K*-vacancy is independent of the kinetic energy and is enhanced by more than 95% as compared to the cases of no-*K*-vacancy ions. No obvious Doppler shift of the X-rays was observed with the increasing of the kinetic energy.

Author Contributions: Conceptualization, Z.S. and L.C.; methodology, Z.S.; experiments and discussion: J.X., Y.F., B.Z., W.W., J.L., C.S., D.Y. and Y.G.; original draft preparation, X.L., L.C. and Z.S.; review and editing, L.C., M.Z. and Z.S. All authors have read and agreed to the published version of the manuscript.

Funding: This research was funded by the National Nature Science Foundation of China through Grant Nos. 12075291, 11675279, and 12275113.

Data Availability Statement: Not applicable.

Conflicts of Interest: The authors declare no conflict of interest.

References

- Briand, J.P.; De Billy, L.; Charles, P.; Essabaa, S.; Briand, P.; Geller, R.; Desclaux, J.P.; Bliman, S.; Ristori, C. Production of hollow atoms by the excitation of highly charged ions in interaction with a metallic surface. *Phys. Rev. Lett.* **1990**, *65*, 159–162. [[CrossRef](#)]
- Arnau, A.; Aumayr, F.; Echenique, P.M.; Grether, M.; Heiland, W.; Limburg, J.; Morgenstern, R.; Roncin, P.; Schippers, S.; Schuch, R.; et al. Interaction of slow multicharged ions with solid surfaces. *Surf. Sci. Rep.* **1997**, *27*, 117–239. [[CrossRef](#)]
- Schenkel, T.; Hamza, A.V.; Barnes, A.V.; Schneider, D.H. Interaction of slow, very highly charged ions with surfaces. *Prog. Surf. Sci.* **1999**, *61*, 23–84. [[CrossRef](#)]
- Wilhelm, R.A.; El-Said, A.S.; Krok, F.; Heller, R.; Gruber, E.; Aumayr, F.; Facsko, S. Highly charged ion induced nanostructures at surfaces by strong electronic excitations. *Prog. Surf. Sci.* **2015**, *90*, 377–395. [[CrossRef](#)]
- El-Said, A.S.; Heller, R.; Meissl, W.; Ritter, R.; Facsko, S.; Lemell, C.; Solleder, B.; Gebeshuber, I.C.; Betz, G.; Toulemonde, M.; et al. Creation of nanohillocks on CaF₂ surfaces by single slow highly charged ions. *Phys. Rev. Lett.* **2008**, *100*, 237601. [[CrossRef](#)] [[PubMed](#)]
- Schulz-Ertner, D.; Tsujii, H. Particle radiation therapy using proton and heavier ion beams. *J. Clin. Oncol.* **2007**, *25*, 953–964. [[CrossRef](#)]
- Parks, D.C.; Stöckli, M.P.; Bell, E.W.; Ratliff, L.P.; Schmieder, R.W.; Serpa, F.G.; Gillaspay, J.D. Non-kinetic damage on insulating materials by highly charged ion bombardment. *Nucl. Instrum. Methods Phys. Res. B* **1998**, *134*, 46. [[CrossRef](#)]
- Hagstrum, H.D. Auger ejection of electrons from tungsten by noble gas ions. *Phys. Rev.* **1954**, *96*, 325. [[CrossRef](#)]
- Arifov, U.; Kishinev, L.M.; Mukhamad, E.S.; Parilis, E. Auger-neutralization of multicharged ions in a metal surface. *Phys. Technol. Phys.* **1973**, *18*, 240.
- Burgdörfer, J.; Lerner, P.; Meyer, F.W. Above-surface neutralization of highly charged ions: The classical over-the-barrier model. *Phys. Rev. A* **1991**, *44*, 5674. [[CrossRef](#)] [[PubMed](#)]
- Nedeljković, N.N.; Majkić, M.D. Intermediate stages of the Rydberg-level population of multiply charged ions escaping solid surfaces. *Phys. Rev. A* **2007**, *76*, 042902. [[CrossRef](#)]
- Nedeljković, N.N.; Nedeljković, L.D.; Mirković, M.A. Electron capture into large-*l* Rydberg states of multiply charged ions escaping from solid surfaces. *Phys. Rev. A* **2003**, *68*, 012721. [[CrossRef](#)]
- Nedeljković, N.N.; Majkić, M.D.; Božanić, D.K.; Dojčilović, R.J. Dynamics of the Rydberg state population of slow highly charged ions impinging a solid surface at arbitrary collision geometry. *J. Phys. B At. Mol. Opt. Phys.* **2016**, *49*, 125201. [[CrossRef](#)]
- Machicoane, G.A.; Schenkel, T.; Niedermayr, T.R.; Newmann, M.W.; Hamza, A.V.; Barnes, A.V.; McDonald, J.W.; Tanis, J.A.; Schneider, D.H. Internal dielectronic excitation in highly charged ions colliding with surfaces. *Phys. Rev. A* **2002**, *65*, 042903. [[CrossRef](#)]
- Hell, N.; Beiersdorfer, P.; Brown, G.V.; Eckart, M.E.; Kelley, R.L.; Kilbourne, C.A.; Leutenegger, M.A.; Lockard, T.E.; Porter, F.S.; Wilms, J. Highly charged ions in a new era of high resolution X-ray astrophysics. *X-ray Spectrom.* **2020**, *49*, 218. [[CrossRef](#)]
- Knapen, J.H.; Erroz-Ferrer, S.; Roa, J.; Bakos, J.; Cisternas, M.; Leaman, R.; Szymanek, N. Optical imaging for the Spitzer Survey of Stellar Structure in Galaxies Data release and notes on interacting galaxies. *Astron. Astrophys.* **2014**, *569*, A91. [[CrossRef](#)]
- Aharonian, F.; Akamatsu, H.; Akimoto, F.; Allen, S.W.; Angelini, L.; Audard, M.; Awaki, H.; Axelsson, M.; Bamba, A.; Bautz, M.W.; et al. Solar abundance ratios of the iron-peak elements in the Perseus cluster. *Nature* **2017**, *551*, 478.
- Beiersdorfer, P. Laboratory X-ray astrophysics. *Ann. Rev. Astron. Astrophys.* **2003**, *41*, 343. [[CrossRef](#)]
- Zhang, B.Z.; Song, Z.Y.; Liu, X.; Qian, C.; Fang, X.; Shao, C.J.; Wang, W.; Liu, J.L.; Xu, J.K.; Feng, Y.; et al. K-shell ionization of 25–100 keV N^{q+} (*q* = 3, 5) ions impinging on Al and Cu surfaces. *Eur. Phys. J. D* **2022**, *76*, 49. [[CrossRef](#)]
- Wang, W.; Song, Z.Y.; Zhang, B.Z.; Liu, X.; Qian, C.; Fang, X.; Shao, C.J.; Liu, J.L.; Zhang, M.W.; Xu, J.K.; et al. K-X-ray emission of 1.5–20 keV/*q* O^{q+} (*q* = 3, 5, 6) and N^{q+} (*q* = 3, 5) ions impinging on nickel surface. *Eur. Phys. J. Plus.* **2022**, *137*, 1015. [[CrossRef](#)]
- Chen, X.M.; Shao, J.X.; Yang, Z.H.; Zhang, H.Q.; Cui, Y.; Xu, X.; Xiao, G.Q.; Zhao, Y.T.; Zhang, X.A.; Zhang, Y.P. K-shell ionization cross section of aluminium induced by low-energy highly charged argon ions. *Eur. Phys. J. D* **2007**, *41*, 281. [[CrossRef](#)]

22. Hubbell, J.H.; Trehan, P.N.; Singh, N.; Chand, B.; Mehta, D.; Garg, M.L.; Garg, R.R.; Singh, S.; Puri, S. A review, bibliography, and tabulation of K, L, and higher atomic shell X-ray fluorescence yields. *J. Phys. Chem. Ref. Data* **1994**, *23*, 339.
23. Ziegler, J.F.; Ziegler, M.D.; Biersack, J.P. SRIM—The stopping and range of ions in matter (2010). *Nucl. Inst. Meth. Phys. B* **2010**, *268*, 1818. [[CrossRef](#)]
24. McGuire, J.H.; Richard, P. Procedure for computing cross sections for single and multiple ionization of atoms in the Binary-encounter approximation by the impact of heavy charged particles. *Phys. Rev. A* **1973**, *8*, 1374. [[CrossRef](#)]